Experimental Hematology

Experimental Hematology 2019;72:60–71

REGULAR SUBMISSION

# Vorinostat synergizes with antioxidant therapy to target myeloproliferative neoplasms

Bruno A. Cardoso[a,b], Teresa L. Ramos[a,c], Hélio Belo[a,b], Filipe Vilas-Boas[d], Carla Real[d], and António M. Almeida[a,b,e]

[a]*Unidade de Investigação em Patobiologia Molecular, Instituto Português de Oncologia de Lisboa Francisco Gentil, E.P.E, Lisboa, Portugal;* [b]*Centro de Estudos de Doenças Crónicas, CEDOC, NOVA Medical School/Faculdade de Ciências Médicas, Universidade Nova de Lisboa, Lisboa, Portugal;* [c]*Universidad de Salamanca-IBSAL-Hospital Universitario, Servicio de Hematología, Salamanca, Spain;* [d]*Centro de Química e Bioquímica, Faculdade de Ciências, Universidade de Lisboa, Lisboa, Portugal;* [e]*Hospital da Luz, Lisboa, Portugal*

(Received 15 October 2018; revised 7 February 2019; accepted 9 February 2019)

**BCR-ABL-negative myeloproliferative neoplasms (MPNs) are driven by JAK-STAT pathway activation, but epigenetic alterations also play an important pathophysiological role. These can be pharmacologically manipulated with histone deacetylase inhibitors (HDACIs), which have proven to be clinically effective in the treatment of MPNs but exhibit dose-limiting toxicity. The treatment of primary MPN cells with vorinostat modulates the expression of genes associated with apoptosis, cell cycle, inflammation, and signaling. The induction of this transcriptional program results in decreased cellular viability, paralleled by a decrease in levels of reactive oxygen species (ROS). In vitro manipulation of ROS levels revealed that the reduction of ROS levels promoted apoptosis. When vorinostat was combined with antioxidant agents, the apoptosis of MPN cells increased in a synergistic manner. The results described here suggest a novel and promising therapeutic strategy combining HDACIs with ROS-reducing agents to treat MPNs. © 2019 Published by Elsevier Inc. on behalf of ISEH – Society for Hematology and Stem Cells.**

The classic BCR-ABL-negative myeloproliferative neoplasms (MPNs) include polycythemia vera (PV), essential thrombocytosis (ET), and primary myelofibrosis (PMF). These are clonal conditions that arise in myeloid precursor cells and result in the increased proliferation of erythroid and megakaryocytic lineages and in the deregulation of bone marrow (BM) architecture and homeostasis [1]. The major clinical complications associated with these disorders are thrombohemorrhagic events, splenomegaly, constitutional symptoms, and transformation to acute myeloid leukemia (AML). Bone marrow transplantation is the only currently available curative therapy [2].

The seminal discovery of the gain-of-function mutation in the tyrosine kinase encoded by the human *JAK2* gene resulting in a valine-to-phenylalanine substitution at the codon 617 (*JAK2V617F*) identified a common genetic basis for the three different conditions [3–6]. This discovery paved the way for the introduction of JAK2 inhibitors into clinical practice [7,8]. However, this targeted treatment modality failed to consistently reduce tumor burden [9], suggesting that other mechanisms may be implicated in MPN disease pathophysiology.

Epigenetic modifications, such as DNA methylation and histone acetylation, are pivotal mechanisms by which cells regulate gene expression [10,11]. Increasing evidence has revealed that these mechanisms play crucial roles in

AMA and BAC designed the research and study. BAC, TLR, HB and FVB performed the research. BAC, FVB, CR and AMA analyzed and interpreted the data. AMA and BAC wrote the manuscript.

Offprint requests to: António Medina Almeida, Department of Haematology, Instituto Português de Oncologia de Lisboa Francisco Gentil, Rua Prof. Lima Basto, 1090-023 Lisbon, Portugal; E-mail: amalmeida@ipolisboa.min-saude.pt

Supplementary material associated with this article can be found, in the online version, at https://doi.org/10.1016/j.exphem.2019.02.002.

0301-472X/© 2019 Published by Elsevier Inc. on behalf of ISEH – Society for Hematology and Stem Cells.
https://doi.org/10.1016/j.exphem.2019.02.002

oncogenesis. Epigenetic modifications can be pharmacologically manipulated by the use of DNA hypomethylating agents and histone deacetylase inhibitors (HDACIs) [12–14]. In past years, these agents have emerged as innovative anti-cancer drugs either in monotherapy, for example, with vorinostat [15,16] and azacitidine [17], or in combinations [18].

Vorinostat is an HDACI currently approved for the treatment of cutaneous T-cell lymphoma [16] and has proven to be effective in a wide variety of hematological malignancies, both in vitro [19,20] and in vivo [21].

In MPNs, vorinostat has been reported to induce apoptosis *in vitro* and to reduce tumor burden in *in vivo* models of MPN [22]. However, the specific effect of vorinostat on whole BM cells and other hematopoietic lineages, as well as the transcriptional program activated on incubation with this agent, is still far from being understood, particularly in the MPN context. In clinical trials, vorinostat reduced tumor burden but resulted in severe toxicity, which limited its tolerability [23].

In an effort to explain the mechanisms by which vorinostat may act in MPN, we identified a previously unrecognized pathway of vorinostat-induced apoptosis. The fact that vorinostat treatment in MPN decreased intracellular reactive oxygen species (ROS) levels opened the possibility of combining ROS-reducing agents and vorinostat to potentiate the anti-tumoral effects in the MPN context.

## Methods

*Primary patient samples and cell line culture*

MPN patient bone marrow (BM) samples were obtained at the Hematology Service of the Instituto Português de Oncologia de Lisboa—Francisco Gentil E.P.E. in the course of routine clinical investigations and following written informed consent. Ethics approval (ethics committee of Instituto Português de Oncologia de Lisboa—Francisco Gentil E.P.E., Approval No. UIC 1018) was obtained, and all samples were treated anonymously in accordance with the Declaration of Helsinki. MPN patient characteristics and information (diagnosis, gender, age, and presence of driver mutations) are summarized in Table 1. Mononuclear cells from BM samples were separated by density gradient centrifugation and cultured in IMDM medium (Sigma-Aldrich, Sintra, Portugal) supplemented with 10% fetal bovine serum (FBS) (Life Technologies), penicillin/streptomycin (Lonza, Cologne, Germany), and L-glutamine (Life Technologies, Carlsbad, CA, USA).

The MPN cell lines HEL, SET-2, and UKE-1 were kindly donated by Professor Jean Luc-Villeval [24,25]. The HEL and SET-2 cell lines were cultured in RPMI-1640 medium (Life Technologies) supplemented with 10% FBS and penicillin/streptomycin. The UKE-1 cell line was cultured in IMDM medium supplemented with 10% FBS, penicillin/streptomycin and L-glutamine. The human BM stromal cell line HS-5 was kindly donated by Professor Paolo Gia [26] and was maintained in IMDM medium supplemented with 10% FBS, penicillin/streptomycin, and L-glutamine.

When indicated, the pharmacological reagents vorinostat (Selleckchem, Houston, TX, USA); ruxolitinib (Axon Medchem, Groningen, The Netherlands); diphenyleneiodonium (Sigma-Aldrich); vitamin C (Sigma-Aldrich); naringenin (Sigma-Aldrich); 3-aminotriazole (Sigma-Aldrich); and Z-Vad-FMK (Enzo Life Sciences, Farmingdale, NY, USA) were added to the cellular culture with MPN primary samples or cell lines. At the indicated time points, the cells were harvested and assessed as described below for cellular viability, intracellular ROS levels, and gene expression.

*In vitro coculture assays*

The in vitro coculture assays were performed as previously described [27]. Briefly, HS-5 cells were cultured to 70% confluence, and the SET-2 cells added to the stromal layer of HS-5 at $0.1 \times 10^6$ cells/mL. In parallel, MPN cells were incubated without any stromal support (no stroma). Vorinostat (Selleckchem), SP600125 (JNK inhibitor, Selleckchem) LY294002 (PI3K inhibitor, Cayman Chemicals, Ann Arbor, MI, USA), ascorbic acid (Sigma-Aldrich), and naringenin (Sigma-Aldrich) were added to the cocultures once the MPN cells adhered to the HS-5 stroma. At 72 hours of coculture, the cells were harvested and assessed as described below for cellular viability.

*Analysis of cellular viability*

When indicated, cultured MPN cells (cell lines and primary patient samples) were harvested, stained with CD45-APC (Biolegend, San Diego, CA, USA) to distinguish the different hematopoietic lineages and from non-hematopoietic cells,

**Table 1.** Characteristics of patients with myeloproliferative neoplasms.

| Patient | Diagnosis | Gender | Age at diagnosis | Hb (g/dL) | WBC ($10^3/\mu L$) | Platelets ($10^3/\mu L$) | Driver mutation |
|---|---|---|---|---|---|---|---|
| 1 | ET | M | 79 | 17.4 | 13,700 | 1310 | *JAK2V617F* |
| 2 | ET | F | 38 | 14.2 | 14,100 | 833 | *JAK2V617F* |
| 3 | ET | M | 50 | 12.7 | 10,800 | 752 | *JAK2V617F* |
| 4 | ET | M | 83 | 16.0 | 32,800 | 961 | Unknown[a] |
| 5 | PV | F | 56 | 13.5 | 11,900 | 907 | *JAK2V617F* |
| 6 | ET | F | 36 | 12.4 | 9,160 | 566 | Unknown |

*ET*=essential thrombocytosis; *Hb*=hemoglobin levels; *PV*=polycythemia vera; *WBC*=white blood cell count.
[a]Unknown indicates that the driver mutation was not identified with the current laboratory tests.

and finally stained with Annexin-V–fluorescein isothiocyanate (FITC, Biolegend) and propidium iodide (PI, Sigma-Aldrich) using standard protocols. Flow cytometric data were acquired on a FACSCalibur flow cytometer (BD Biosciences, San Jose, CA, USA), and the percentage of viable cells was described as those that did not stain for Annexin-V and PI. Viability was also assessed by PI exclusion analysis by flow cytometry. The data were analyzed using Flow Jo software, Version X.0.7 (Tree Star Inc., Ashland, OR, USA).

*Determination of intracellular ROS levels*

Levels of intracellular ROS were measured as previously described [28]. Briefly, under the described culture conditions, the cells were harvested and incubated with 10 $\mu$mol/L dichlorofluorescein diacetate (DCF-DA) (Sigma-Aldrich) for 30 min at 37°C, washed, and analyzed by flow cytometry as described previously.

*Drug titration and interaction analysis*

SET-2 cells were cultured for 72 hours in the presence of the following pharmacological reagents that were incubated alone and in combinations: vorinostat (#1) with ascorbic acid (#2) and vorinostat (#1) with naringenin (#3). The agents were added to these cultures in the concentrations described in Supplementary Table S1 (online only, available at www.exphem.org), and cellular viability was analyzed as described previously. The half-maximal effective concentration ($EC_{50}$) calculation was performed using GraphPad Prism Version 5.0.0 for Windows (GraphPad Software, San Diego, CA, USA), and drug interactions were calculated using the Chou–Talalay method [29]. Furthermore, drug interaction was assessed using the coefficient of drug interaction (CDI) [30] when vorinostat and vitamin C or naringenin were combined at defined concentrations. The CDI is calculated as $CDI = AB/(A \times B)$, where $AB$ is the viability index of the drug combination, and $A$ and $B$ are the viability indexes of the drugs used as single agents.

*RNA extraction, RT-PCR, and quantitative RT-PCR*

RNA was extracted as previously described [27,31]. cDNA was synthesized and gene expression evaluated by quantitative real-time polymerase chain reaction (qPCR) and normalized to the expression levels of *HPRT1* gene. Primers used for the qPCR are available on request. The reagents were combined according to standard protocols, and the amplifications performed in a LightCycler 480 II thermocycler (Roche, Mannhein, Germany). In Supplementary Tables S2 and S3 (online only, available at www.exphem.org), the relative levels of each transcript were normalized to the levels of each control condition (0.0 $\mu$mol/L vorinostat) and depicted as a logarithm of base 2.

*Statistical analysis*

Differences between populations were analyzed with an unpaired two-tailed Student $t$ test or a one-way analysis of variance (ANOVA), when appropriate, using GraphPad Prism version 5.0.0 for Windows (GraphPad Software). A $p$ value $< 0.05$ was considered to indicate significance.

## Results

*Vorinostat impairs cellular viability and ROS levels in MPN*

We start by investigating the functional effects of vorinostat in MPN cells. The treatment of mononuclear cells isolated from BM samples collected from diagnosed MPN patients (Table 1) with a clinically relevant dose of vorinostat [32] resulted in a modest increase in apoptosis (Figure 1A). These results led us to hypothesize that vorinostat might have differential effects on the several blood lineages. To address this, we use the gating strategy demonstrated in Figure 1B and Supplementary Figure E1A (online only, available at www.exphem.org), which allows discrimination between monocytes, granulocytes, lymphocytes, progenitors, and erythrocytes. Analysis of apoptosis within the different hematopoietic populations revealed that vorinostat affects preferentially the monocyte and granulocyte lineages and, to a lesser extent, the progenitor population (Figure 1B; Supplementary Figure S1, online only, available at www.exphem.org).

The treatment of MPN cell lines (UKE-1, HEL, and SET-2) with vorinostat also decreased cellular viability (Figure 2A) in a time (Figure 2B)- and dose-dependent manner (Supplementary Figure S2, online only, available at www.exphem.org). Moreover, the treatment of SET-2 with other HDACIs (trichostatin A, butyric acid, and romidepsin) also resulted in decreased viability (Supplementary Figure S3A, online only, available at www.exphem.org).

*Vorinostat modulates the expression of apoptotic and signaling genes in MPN cells*

Next we assessed the impact of vorinostat on the transcriptional profile of MPN cells at two different time points, 8 hours (early time point) and 24 hours (late time point). We analyzed the expression of a panel of genes that are associated with apoptosis, cell cycle and proliferation, kinases, and signaling (Supplementary Tables S2–S4, online only, available at www.exphem.org).

The treatment of SET-2 cells with vorinostat altered the expression of 37% of the genes analyzed (58 of 156 genes altered their expression). The majority of genes are upregulated in response to vorinostat (Supplementary Tables S2 and S3), including the canonical HDACI target, *CDKN1A* [19,27,31,33] (Supplementary Figure S4, online only, available at www.exphem.org).

Vorinostat also decreased the expression of JAK-STAT target genes (Supplementary Tables S2, S3 and Supplementary Figure S5A, online only, available at www.exphem.org). Furthermore, as outlined in Supplementary Tables S2 and S3, the majority of genes altered by the treatment of SET-2 cells with vorinostat

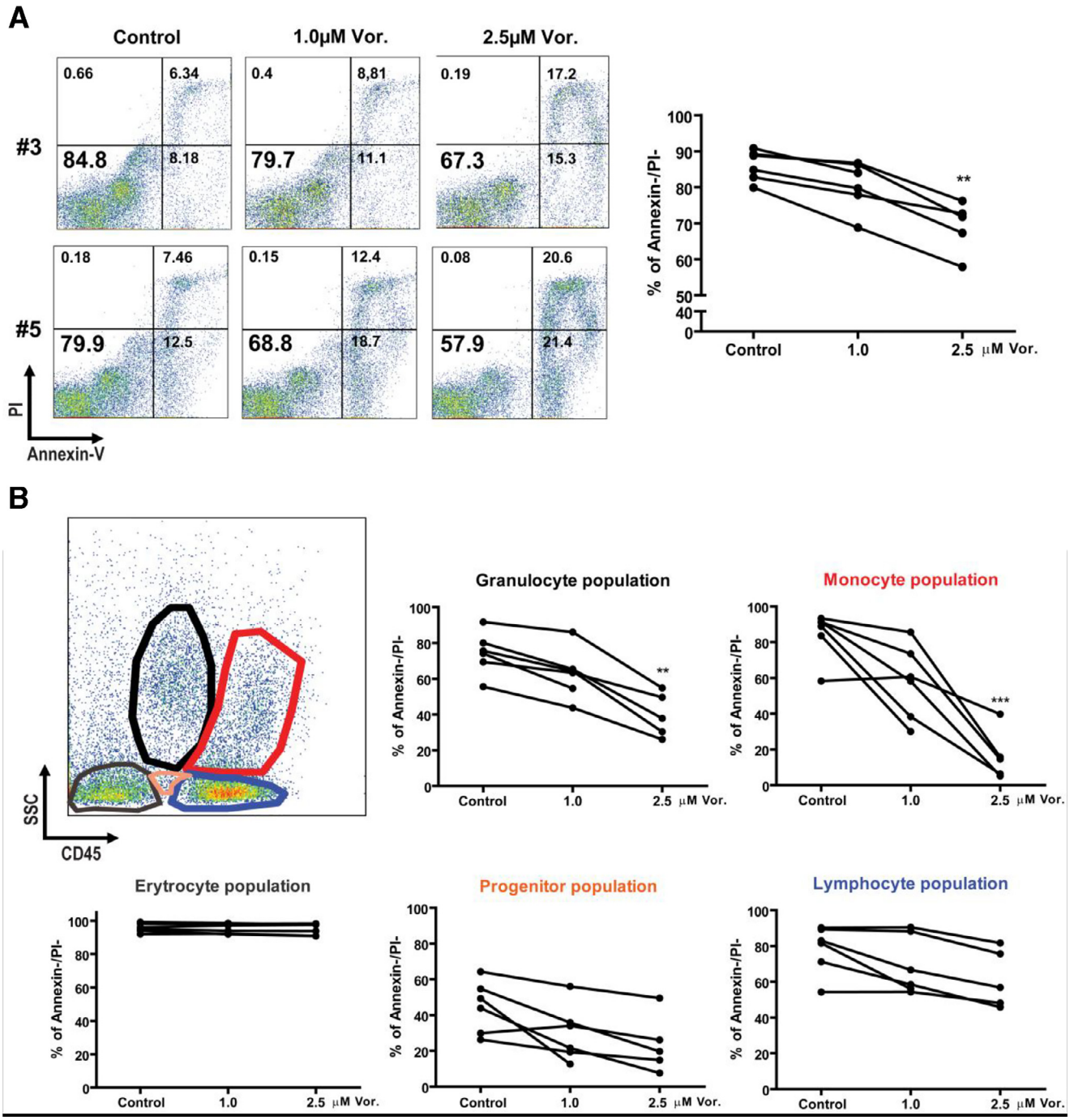


**Figure 1. Vorinostat reduces cellular viability in MPN patient samples.** Patient BMNCs were isolated by Ficoll gradient and cultured with the indicated concentrations of vorinostat. At 72 hours of culture, the cells were harvested and stained as described under Methods to determine cellular viability. (**A**) The left panels show the dot-plots of Annexin-V/PI staining within the whole population of BMNCs of patients 3 and 5. The right graphic indicates percentage of viable cells (Annexin-V/PI) within whole BMNCs in all the MPN patients analyzed ($n = 6$). (**B**) By using SSC versus CD45 gating strategy (left dot-plot) we were able to distinguish five different hematopoietic lineages (monocytes, granulocytes, lymphocytes, progenitors, and erythrocytes) and we determined cellular viability within these populations all the MPN patients. The graphics indicate the percentage of viable cells (Annexin-V/PI) in each condition within the different lineages for each patient analyzed ($n = 6$). $^{**}p < 0.01$; $^{***}p < 0.001$. *BMNCs*=bone marrow mononuclear cells; *MPN*=myeloproliferative neoplasms; *PI*=propidium iodide; *SSC*=side scatter; *Vor.* =vorinostat.

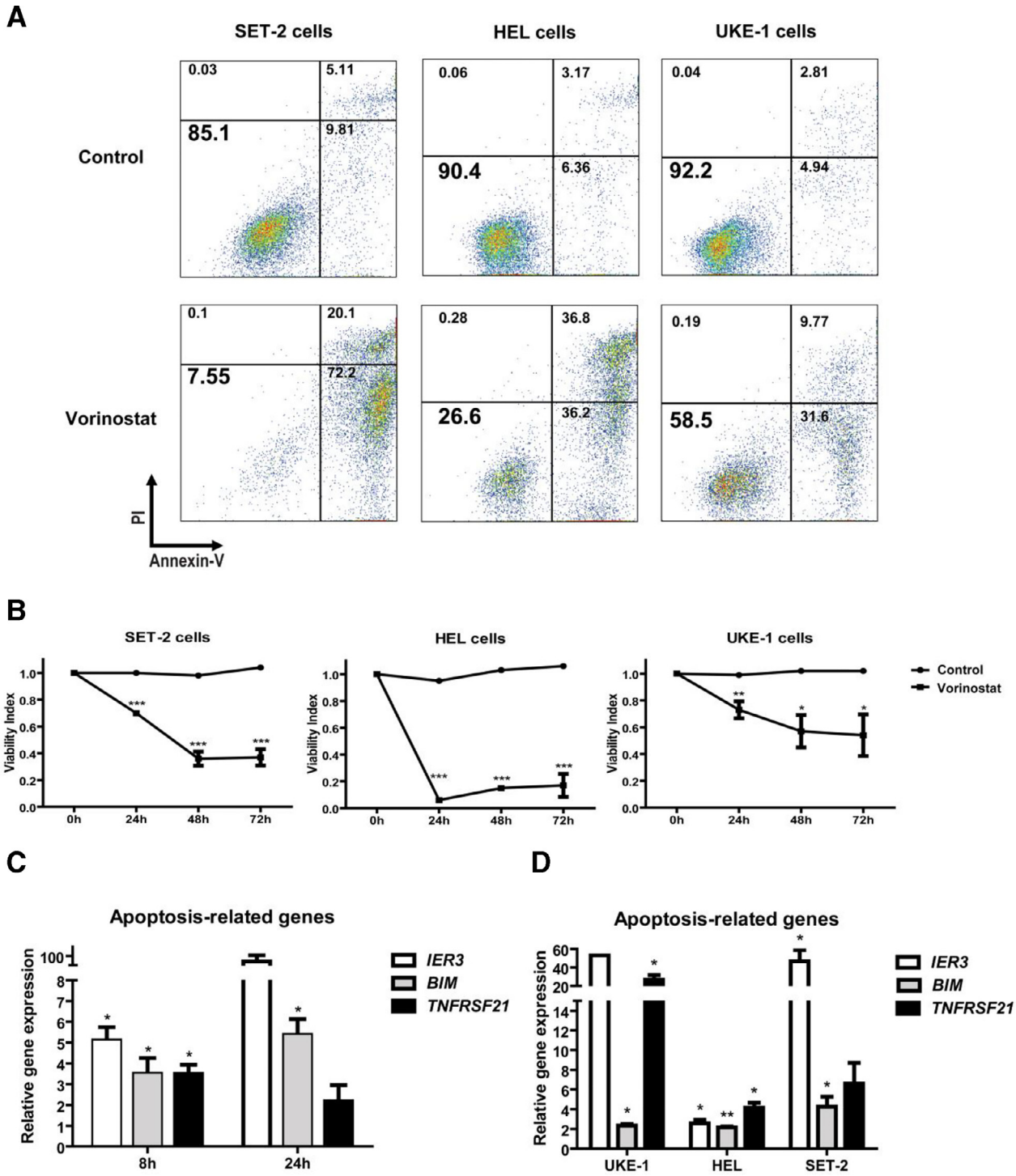


**Figure 2. Vorinostat reduces cellular viability and activates "apoptotic" genes in MPN cell lines.** (**A**) MPN cell lines UKE-1, HEL, and SET-2 were cultured in vitro with vorinostat (2.5 $\mu$mol/L). At 72 hours of culture, the cells were harvested and stained with Annexin-V/PI to determine cellular viability by flow cytometry. The panels are dotplots of the Annexin-V/PI staining under the different conditions. (**B**) MPN cell lines UKE-1, HEL, and SET-2 were cultured in vitro with vorinostat (2.5 $\mu$mol/L). At the indicated time points, the cells were harvested and stained as described under Methods to determine cellular viability. The viability index normalizes the viability values to those of the 0-hour time point. (**C**) SET-2 cells were cultured with 2.5 $\mu$mol/L vorinostat, and at the indicated time point, the cells were lysed for RNA extraction. (**D**) MPN cell lines UKE-1, HEL, and SET-2 were cultured for 24 hours with 2.0 $\mu$mol/L vorinostat and lysed for RNA extraction. Transcript levels of the indicated genes were evaluated as described under Methods, and the values of each gene were normalized to *HPRT1* and depicted as relative values of the control condition (0.0 $\mu$mol vorinostat). Values are expressed as the mean ± standard deviation of at least three experiments. *$p < 0.05$; **$p < 0.01$; ***$p < 0.001$. *MPN*=myeloproliferative neoplasms; *PI*=propidium iodide.

are associated with apoptosis and signaling and also encode for transcription factors relevant for hematopoiesis. These results were validated by qPCR in three different MPN cell lines (SET-2, HEL, and UKE-1). As illustrated in Figure 2C and 2D, vorinostat incubation in MPN cells increases the expression of genes associated with apoptosis (*IER3, BIM,* and *TNFRSF21*) and signaling (*HEY2, DAB2, TNFRSF16,* and *WNT4;* Supplementary Figure S5B, S5C). These results strongly indicate, at least with respect to gene expression, that vorinostat might be effective in targeting MPN cells, both by modulating apoptosis and by suppressing the JAK-STAT signaling pathway.

*Vorinostat impacts on ROS levels in MPN cells*

One of the most documented effects of vorinostat and other HDACIs in cancer cells is the increase in ROS with subsequent increase in DNA damage that eventually leads to apoptosis [34–38]. On this basis, we used primary MPN samples and analyzed ROS levels. Interestingly, and in contrast to previous reports, vorinostat decreased ROS levels in all the patient samples that we analyzed (Figure 3A). Moreover, by using the same gating strategy as in Figure 1B, we observed that the decrease in ROS levels induced by vorinostat was more pronounced in the granulocytic and monocytic lineages (Figure 3B; Supplementary Figure S6, online only, available at www.exphem.org), in consonance with the induction of apoptosis by the vorinostat treatment (Figure 1B). In addition, the incubation of SET-2 cells with other HDACIs (trichostatin A, butyric acid, and romidepsin) also decreased ROS levels (Supplementary Figure S3B). These results indicate that incubation of vorinostat and other HDACIs induces apoptosis in MPN cells and decreases ROS levels.

*Downregulation of ROS levels is required for vorinostat-induced apoptosis*

The results (Figures 1 and 3) suggest that the kinetics of downregulation of both cellular viability and ROS might be linked. To understand whether vorinostat (and also other HDACIs)-induced cell death and the decrease in ROS levels were associated events, we used two alternative strategies.

First, we incubated SET-2 cells with vorinostat and a pan-caspase inhibitor (Z-VAD-FMK), which partially rescued vorinostat-induced cell death (Figure 4A, left panel), but had no effect on ROS levels (Figure 4A, right panel). This suggests that the decrease in ROS levels mediated by vorinostat incubation is not a mere consequence of increased cell death, but rather an independent event.

Second, we modulated ROS levels by using the catalase inhibitor 3-aminotriazole and analyzed its effect on vorinostat-induced cell death. As illustrated in Figure 4B (left panel), incubation with 3-aminotriazole (a catalase inhibitor) partially rescued vorinostat-induced cell death, an effect concomitant with an increase in ROS levels (Figure 4B, right panel). These results suggest that the decrease in ROS levels on vorinostat treatment is not a mere consequence of decreased cellular viability, but rather the mechanism that triggers the apoptotic cascade induced by vorinostat, and possibly other HDACIs, in the MPN context.

*Vorinostat synergizes with agents that lower ROS levels to decrease MPN cellular viability*

To test whether pharmacological reagents that further decrease ROS levels would have a synergistic effect with vorinostat in increasing cell death, we treated SET-2 cells with vorinostat and diphenyleneiodonium (an inhibitor of NAD oxidase, a source of ROS) [39]. As illustrated in Figure 4C, the combined treatment with vorinostat and diphenyleneiodonium is more effective in inducing apoptosis (Figure 4C, left panel) and, to a lesser extent, ROS levels (Figure 4C, right panel) than vorinostat or diphenyleneiodonium treatments alone. Importantly, the same effect was observed on combination of vorinostat and two natural occurring pharmacological agents with antioxidant properties, vitamin C [38,39] and naringenin [40]. As illustrated in Figure 5A and 5B, the combined treatment of SET-2 cells with vorinostat and these antioxidant agents induced higher levels of apoptosis (Figure 5A, B; left panels) and was more effective in reducing ROS levels (Figure 5A, B; right panels) as compared with the single-agent treatments. These results were further confirmed using the Chou–Talalay method [29]. Treatment with the combination of vorinostat and either vitamin C (Supplementary Figure 2A) or naringenin (Supplementary Figure 2B) had synergistic effects (CI < 1.0) in increasing cell death at therapeutically relevant doses of vorinostat ($X < 2.52$ $\mu$mol/L) [32] and reduced the $EC_{50}$ of vorinostat in the SET-2 cell line (3.747–1.524 $\mu$mol/L with vitamin C; 4.026 –1.252 $\mu$mol/L with naringenin).

Recently, we reported that the BM stroma can protect MPN cells from ruxolitinib- and vorinostat-induced cytotoxicity and that this protection was mediated, at least in part, by the activation of JNK and PI3K signaling pathways [27]. Given the fact that antioxidant agents synergistically cooperate with vorinostat to induce apoptosis of MPN cells (Figure 5A, B) we tested whether these agents might also reverse the protective effect of the BM. As illustrated in Figure 5C (left panel), the treatment of SET-2 cells with antioxidants (vitamin C and naringenin) clearly reversed the protection induced by BM to vorinostat-induced cytotoxicity and to levels comparable to those of the pharmacological inhibition of JNK and PI3K signaling

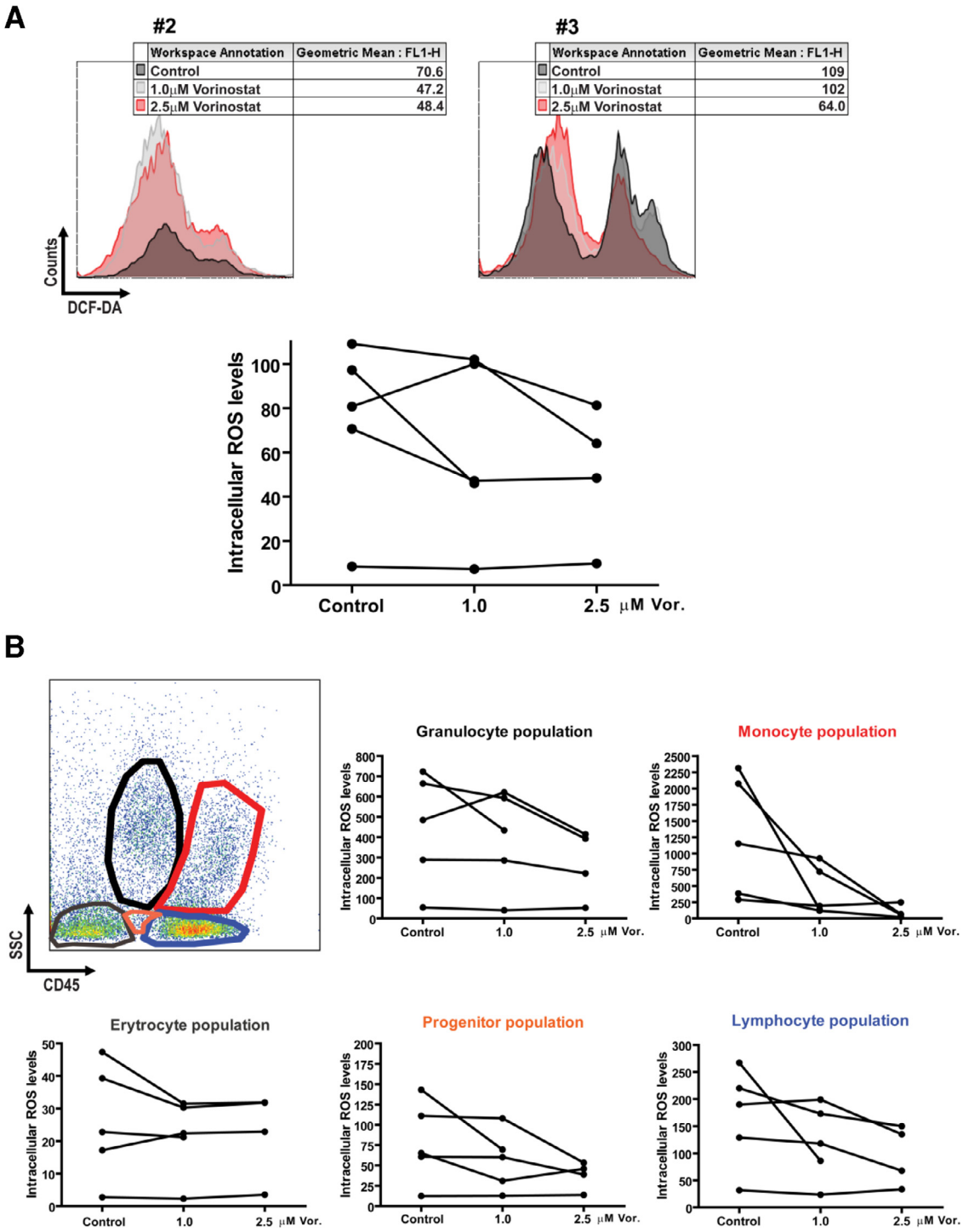


**Figure 3. Vorinostat reduces intracellular levels of ROS in MPN patient samples.** Patient BMNCs were isolated by Ficoll gradient and cultured with the indicated concentrations of vorinostat. At 72 hours of culture, the cells were harvested and stained as described under Methods to determine intracellular ROS levels. (**A**) Histogram plots of intracellular ROS levels within the whole population of BMNCs of patients 2 and 3. (**B**) Intracellular ROS levels (DCF-DA geometric mean intensity) within whole BMNCs in all the MPN patients analyzed ($n = 6$). By using SSC versus CD45 gating strategy (left dotplot), we were able to distinguish five different hematopoietic lineages (monocytes, granulocytes, lymphocytes, progenitors, and erythrocytes), and we determined the intracellular ROS levels in these populations in all the MPN patients. The graphics indicate the intracellular ROS levels (DCF-DA geometric mean) in each condition within the different populations for each patient analyzed ($n = 5$). *BMNCs*=bone marrow mononuclear cells; *DCF-DA*=dichlorofluorescein diacetate; *MPN*=myeloproliferative neoplasms; *PI*=propidium iodide; *ROS*=reactive oxygen species; *SSC*=side scatter; *Vor.*=vorinostat.

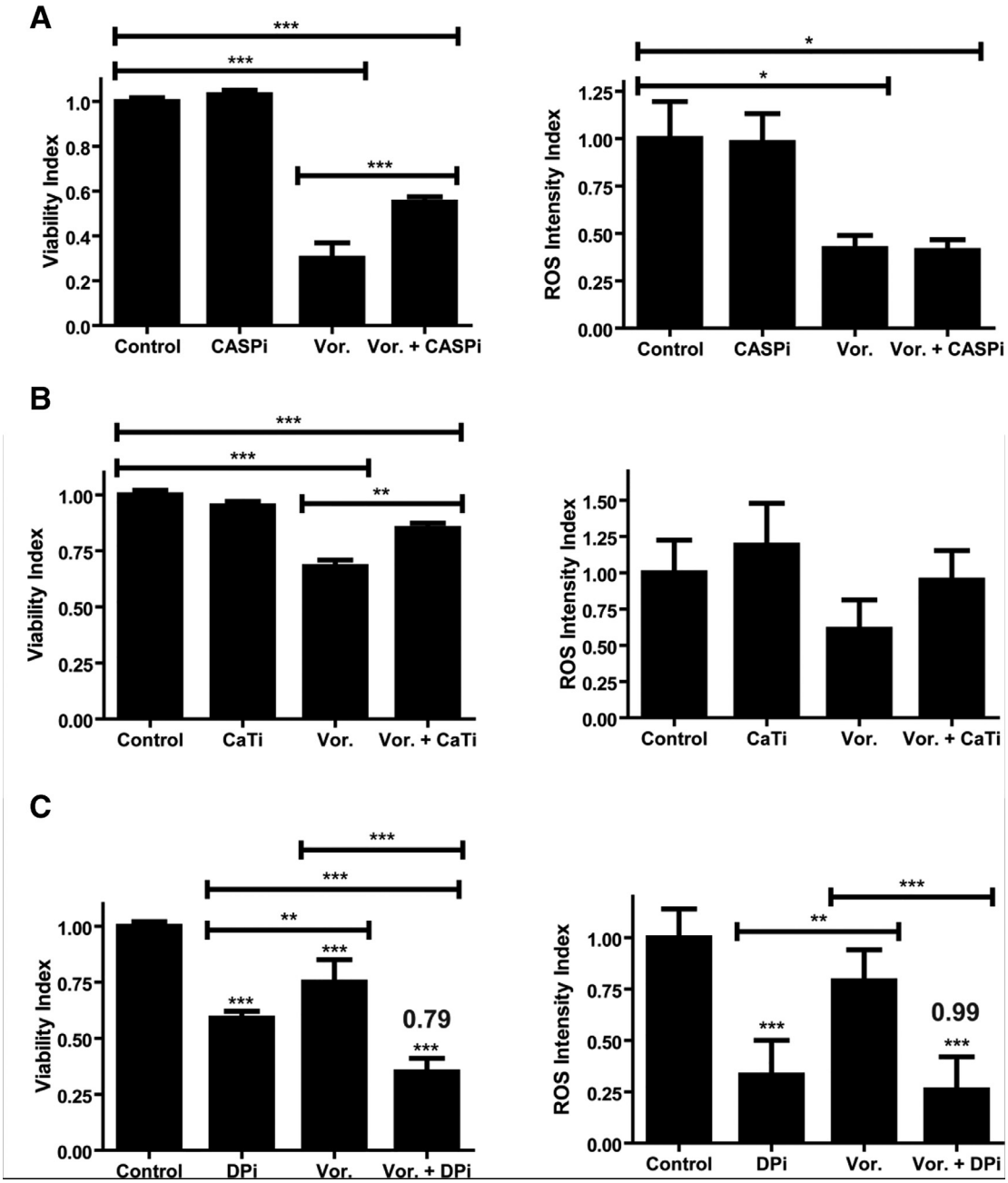


**Figure 4. Vorinostat decreases MPN cellular viability on reduction of intracellular ROS levels.** (**A**) SET-2 cells were cultured in vitro in the presence of control (DMSO), 50 $\mu$mol/L Z-VAD-FMK (CASPi), 2.5 $\mu$mol/L Vor., and both (Vor. + CASPi). At 72 hours, SET-2 cells were harvested and stained as described under Methods to assess cellular viability and intracellular ROS levels. The left graph illustrates the viability index, which normalizes the viability values to those of the control condition (dimethyl sulfoxide). The graph on the right illustrates the ROS intensity index, which normalizes the intracellular ROS levels (dichlorofluorescein diacetate geometric mean) to those of the control condition (DMSO). (**B**) SET-2 cells were cultured in vitro in the presence of control ($H_2O$), 0.01 mol/L CaTi, 1.0 $\mu$mol/L Vor., and both (Vor. + CaTi). At 72 hours, SET-2 cells were harvested and stained as described under Methods to assess cellular viability and intracellular ROS levels. As in (A), the left graph illustrates the viability index, and the right graph, the ROS intensity index, which normalizes the viability and ROS levels to the respective control condition (control = $H_2O$). The values indicated above the bars are the CDIs calculated for each condition. (**C**) SET-2 cells were cultured in vitro in the presence of control ($H_2O$), 10 $\mu$mol/L DPi, 1.0 $\mu$mol/L Vor., and both (Vor. + DPi). At 72 hours, SET-2 cells were harvested and stained as described under Methods to assess cellular viability and intracellular ROS levels. As in (A) and (B), the left graph illustrates the viability index, and the right graph illustrates the ROS intensity index, which normalizes the viability and ROS levels to the respective control condition (control = $H_2O$). Values represent the mean ± standard deviation of at least three experiments. *$p < 0.05$; **$p < 0.01$; ***$p < 0.001$. *CASPi*=caspase inhibitor; *CaTi*=3-aminotriazole; *CDI*=coefficient of drug interaction; *DPi*=diphenyleneiodonum; *MPN*=myeloproliferative neoplasm; *ROS*=reactive oxygen species; *Vor.*=vorinostat.

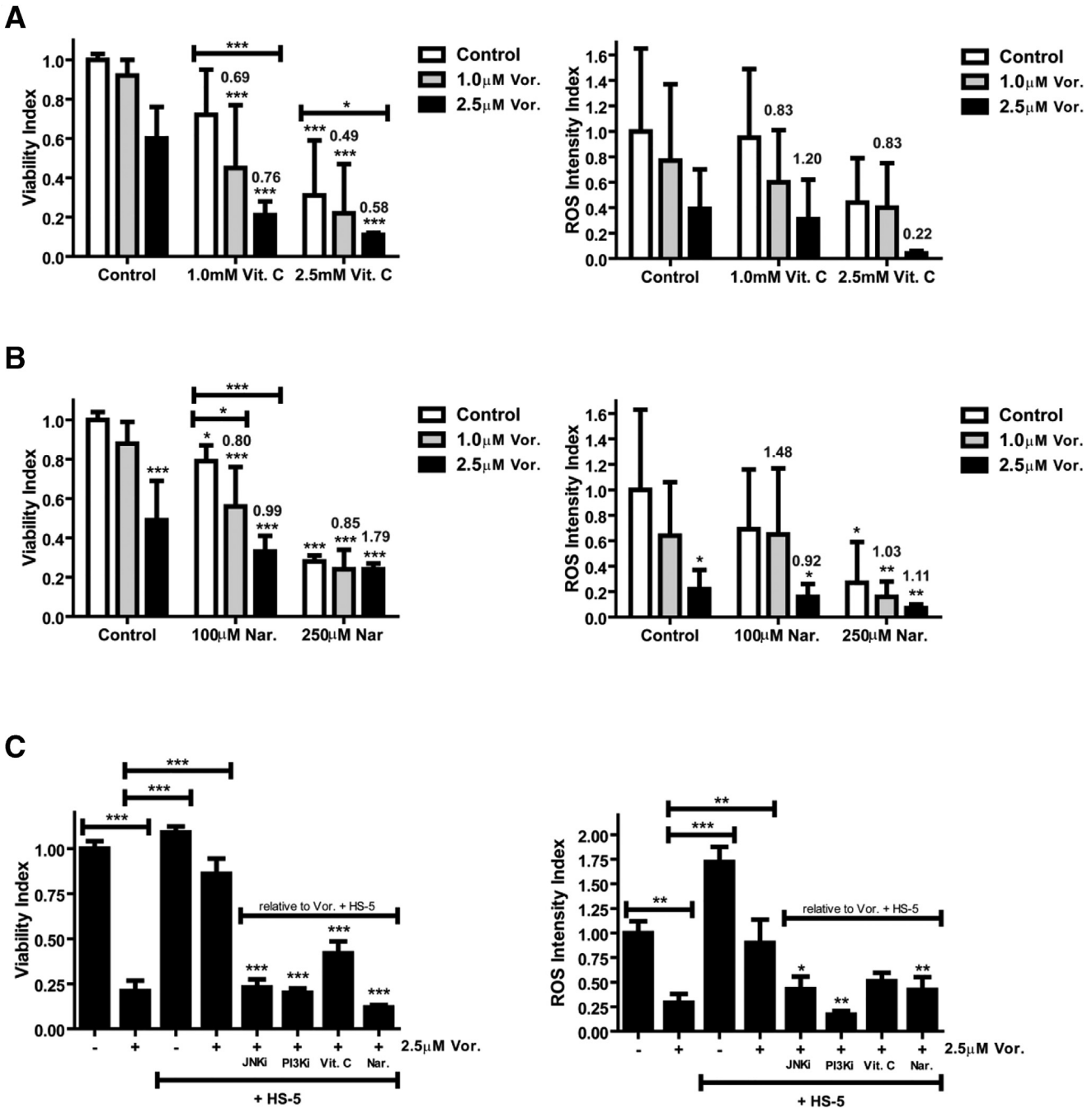


**Figure 5. Inhibition of intracellular ROS levels synergizes with Vor. to induce apoptosis in MPN cells.** (**A, B**) SET-2 cells were cultured in vitro in the presence of the indicated concentrations of the pharmacological agents: (**A**) Control ($H_2O$), Vit. C, Vor., and both (Vor. + Vit. C). (**B**) Control (70% ethanol), Nar., Vor., and both (Vor. + Nar.). At 72 hours, SET-2 cells were harvested and stained as described under Methods to assess cellular viability and intracellular ROS levels. The left graphs illustrate the viability index, which normalizes the viability values to those of the control condition (DMSO). The graphs on the right illustrate the ROS intensity index, which normalizes the intracellular ROS levels (DCF-DA geometric mean) to those of each control condition. (**C**) SET-2 cells were cultured in vitro (no stroma) and cocultured with a stromal layer of HS-5 cells (+ HS-5) in the presence of 2.5 $\mu$M Vor. in monotherapy and in combination with 10 $\mu$mol/L SP600125 (JNKi), 10 $\mu$mol/L LY294002 (PI3Ki), 2.5 mmol/L Vit. C, 250 $\mu$mol/L Nar. At 72 hours of culture, SET-2 cells were harvested and stained with CD45-APC (to distinguish between SET-2 cells and the HS-5 bone marrow stroma), PI, and DCF-DA to determine cellular viability and intracellular ROS levels as described under Methods. The graph in the left panel illustrates the viability index, and the graph in the right panel illustrates the ROS intensity index, which normalizes the viability values and intracellular ROS levels (DCF-DA geometric mean) to those of the control conditions (non-treated without HS-5 stroma). The values represent the mean ± standard deviation of at least three experiments. *$p < 0.05$; **$p < 0.01$; ***$p < 0.001$. *DCF-DA*=dichlorofluorescein diacetate; *DMSO*=dimethyl sulfoxide; *Nar.*=naringenin; *PI*=propidium iodide; *ROS*=reactive oxygen species; *Vit. C*=vitamin C; *Vor.*=vorinostat.

pathways. We observed the same degree of reversion in ROS levels (Figure 5C, right panel).

Our results indicate that the combination of vorinostat and antioxidant agents induces higher levels of MPN cell apoptosis and the effect is sufficient to abolish the protection induced by the BM microenvironment [27].

## Discussion

An extensive amount of data collected in past decades indicated the pivotal role of epigenetic modifications (DNA methylation and histone acetylation) in the pathophysiology of hematological malignancies [11,41]. Importantly, these epigenetic modifications are targetable with the use of pharmacological agents, such as DNA hypomethylating agents and HDACIs [14]. The incubation of cancer cells with HDACIs induces changes in the transcriptional program that result in apoptosis and cell cycle arrest in vitro [42]. Furthermore, treatment with such pharmacological agents in vivo resulted in halted tumor growth and led to tumor regression in a variety of human cancer models [12,43], making these agents highly attractive as novel anti-cancer agents [44].

Vorinostat (or suberoylanilide hydroxamic acid) is a general HDACI that is currently used in the clinical treatment of cutaneous T-cell lymphomas [16] and is being investigated for other hematologic malignancies [45].

Vorinostat normalized blood counts in a mouse model of MPN [22]. In a phase II clinical trial with polycythemia vera and essential thrombocytosis patients, vorinostat normalized blood counts and decreased tumor burden, but was associated with significant toxicity and a high discontinuation rate [23].

Our experiments confirm that vorinostat can modulate gene expression [19,42]; in particular, it upregulates *CDKN1A* expression [19,27,31,33], thereby promoting apoptosis [19,22,27,31,37,46].

One of the described mechanisms by which HDACIs induce apoptosis is through the increase in DNA damage, which produces high levels of ROS, triggering the apoptotic process [35,36,47]. However, our experiments indicate for the first time that vorinostat decreases ROS levels in MPN cells. This effect of vorinostat seems to be quite specific to MPN cells, as the treatment of non-MPN cell lines (THP-1 and NB.4) did not alter ROS levels significantly (Supplementary Figure S7, online only, available at www.exphem.org). One possible explanation is that vorinostat might have an impact on enzymes that modulate cellular ROS levels [48]. However we observed no effect of vorinostat on the levels of the *SOD2* gene (Supplementary Figure S8, online only, available at www.exphem.org). Another possible explanation for this observation is the fact that JAK-STAT signaling of activation requires generation of ROS [49–51]. This is corroborated by our observation that JAK2 inhibition of the same cells results in reduction of ROS (Supplementary Figure S9, online only, available at www.exphem.org). Thus, vorinostat could impair JAK-STAT signaling by reducing ROS formation. The observation that HDACI-induced apoptosis relies on the damping of ROS levels led us to hypothesize that combining ROS scavengers with HDACIs could be synergistic in the promotion of MPN cell death. We found that combining ROS reduction with vorinostat treatment resulted in a higher rate of cell death than obtained with the respective treatments alone in a synergistic manner. This could indicate a potential novel combination treatment for MPN.

In summary, we have demonstrated that vorinostat promotes MPN cell death through reduction of ROS. Importantly, by combining vorinostat and ROS-reducing agents, we were able to induce a higher degree of cell death in MPN cells. These results may open a novel therapeutic option for MPN patients.

## Acknowledgments

We are grateful to Professor Jean Luc Villeval and Dr. Paolo Ghia for kindly donating the SET-2, UKE-1, and HS-5 cell lines we used in this study; Clemente da Silva for his technical support; and the patients and their families who generously contributed to this study.

## Conflict of interest disclosure

AMA receives consulting fees from Celgene and Novartis and is on the board of speakers for Bristol-Meyer Squibb, Shire, and Amgen. BAC, TLR, HB, FVB, and CR have no conflicts of interest to declare.

## References

1. Tefferi A, Vainchenker W. Myeloproliferative neoplasms: molecular pathophysiology, essential clinical understanding, and treatment strategies. J Clin Oncol. 2011;29:573–582.
2. Vannucchi AM, Guglielmelli P, Tefferi A. Advances in understanding and management of myeloproliferative neoplasms. CA Cancer J Clin. 2009;59:171–191.
3. Levine RL, Wadleigh M, Cools J, et al. Activating mutation in the tyrosine kinase JAK2 in polycythemia vera, essential thrombocythemia, and myeloid metaplasia with myelofibrosis. Cancer Cell. 2005;7:387–397.
4. Baxter EJ, Scott LM, Campbell PJ, et al. Acquired mutation of the tyrosine kinase JAK2 in human myeloproliferative disorders. Lancet. 2005;365:1054–1061.
5. James C, Ugo V, Le Couédic JP, et al. A unique clonal JAK2 mutation leading to constitutive signalling causes polycythaemia vera. Nature. 2005;434:1144–1148.
6. Kralovics R, Passamonti F, Buser AS, et al. A gain-of-function mutation of JAK2 in myeloproliferative disorders. N Engl J Med. 2005;352:1779–1790.
7. Verstovsek S, Mesa RA, Gotlib J, et al. A double-blind, placebo-controlled trial of ruxolitinib for myelofibrosis. N Engl J Med. 2012;366:799–807.

8. Harrison C, Kiladjian JJ, Al-Ali HK, et al. JAK inhibition with ruxolitinib versus best available therapy for myelofibrosis. N Engl J Med. 2012;366:787–798.
9. Mascarenhas J, Hoffman R. A comprehensive review and analysis of the effect of ruxolitinib therapy on the survival of patients with myelofibrosis. Blood. 2013;121:4832–4837.
10. Jones PA, Baylin SB. The epigenomics of cancer. Cell. 2007;128:683–692.
11. Lehmann U, Brakensiek K, Kreipe H. Role of epigenetic changes in hematological malignancies. Ann Hematol. 2004;83:137–152.
12. Stimson L, Wood V, Khan O, Fotheringham S, La Thangue NB. HDAC inhibitor-based therapies and haematological malignancy. Ann Oncol. 2009;20:1293–1302.
13. Leone G, Voso MT, Teofili L, Lübbert M. Inhibitors of DNA methylation in the treatment of hematological malignancies and MDS. Clin Immunol. 2003;109:89–102.
14. Jain N, Rossi A, Garcia-Manero G. Epigenetic therapy of leukemia: an update. Int J Biochem. Cell Biol. 2009;41:72–80.
15. Marks PA. Discovery and development of SAHA as an anticancer agent. Oncogene. 2007;26:1351–1356.
16. Mann BS, Johnson JR, Cohen MH, Justice R, Pazdur R. FDA approval summary: vorinostat for treatment of advanced primary cutaneous T-cell lymphoma. Oncologist. 2007;12:1247–1252.
17. Fenaux P, Mufti GJ, Hellstrom-Lindberg E, et al. Efficacy of azacitidine compared with that of conventional care regimens in the treatment of higher-risk myelodysplastic syndromes: a randomised, open-label, phase III study. Lancet Oncol. 2009;10:223–232.
18. Laubach JP, Moreau P, San-Miguel JF, Richardson PG. Panobinostat for the treatment of multiple myeloma. Clin Cancer Res. 2015;21:4767–4773.
19. Silva G, Cardoso BA, Belo H, Almeida AM. Vorinostat induces apoptosis and differentiation in myeloid malignancies: genetic and molecular mechanisms. PLoS One. 2013;8:e53766.
20. Belo H, Silva G, Cardoso BA, et al. Epigenetic alterations in Fanconi anaemia: role in pathophysiology and therapeutic potential. PLoS One. 2015;10:e0139740.
21. Siegel D, Hussein M, Belani C, et al. Vorinostat in solid and hematologic malignancies. J Hematol Oncol. 2009;2:31.
22. Akada H, Akada S, Gajra A, et al. Efficacy of vorinostat in a murine model of polycythemia vera. Blood. 2012;119:3779–3789.
23. Andersen CL, McMullin MF, Ejerblad E, et al. A phase II study of vorinostat (MK-0683) in patients with polycythaemia vera and essential thrombocythaemia. Br J Haematol. 2013;162:498–508.
24. Quentmeier H, MacLeod RA, Zaborski M, Drexler HG. JAK2 V617F tyrosine kinase mutation in cell lines derived from myeloproliferative disorders. Leukemia. 2006;20:471–476.
25. Uozumi K, Otsuka M, Ohno N, et al. Establishment and characterization of a new human megakaryoblastic cell line (SET-2) that spontaneously matures to megakaryocytes and produces platelet-like particles. Leukemia. 2000;14:142–152.
26. Roecklein BA, Torok-Storb B. Functionally distinct human marrow stromal cell lines immortalized by transduction with the human papilloma virus E6/E7 genes. Blood. 1995;85:997–1005.
27. Cardoso BA, Belo H, Barata JT, Almeida AM. The bone marrow-mediated protection of myeloproliferative neoplastic cells to vorinostat and ruxolitinib relies on the activation of JNK and PI3K signalling pathways. PLoS One. 2015;10:e0143897.
28. Silva A, Gírio A, Cebola I, Santos CI, Antunes F, Barata JT. Intracellular reactive oxygen species are essential for PI3K/Akt/mTOR-dependent IL-7-mediated viability of T-cell acute lymphoblastic leukemia cells. Leukemia. 2011;25:960–967.
29. Chou TC. Theoretical basis, experimental design, and computerized simulation of synergism and antagonism in drug combination studies. Pharmacol Rev. 2006;58:621–681.
30. Li X, Lin Z, Zhang B, et al. β-Elemene sensitizes hepatocellular carcinoma cells to oxaliplatin by preventing oxaliplatin-induced degradation of copper transporter 1. Sci Rep. 2016;6:21010.
31. Cardoso BA, de Almeida SF, Laranjeira AB, et al. TAL1/SCL is downregulated upon histone deacetylase inhibition in T-cell acute lymphoblastic leukemia cells. Leukemia. 2011;25:1578–1586.
32. Kelly WK, O'Connor OA, Krug LM, et al. Phase I study of an oral histone deacetylase inhibitor, suberoylanilide hydroxamic acid, in patients with advanced cancer. J Clin Oncol. 2005;23:3923–3931.
33. Ocker M, Schneider-Stock R. Histone deacetylase inhibitors: signalling towards p21cip1/waf1. Int J Biochem Cell Biol. 2007;39:1367–1374.
34. Ruefli AA, Ausserlechner MJ, Bernhard D, et al. The histone deacetylase inhibitor and chemotherapeutic agent suberoylanilide hydroxamic acid (SAHA) induces a cell-death pathway characterized by cleavage of Bid and production of reactive oxygen species. Proc Natl Acad Sci USA. 2001;98:10833–10838.
35. Rassool FV, Gaymes TJ, Omidvar N, et al. Reactive oxygen species, DNA damage, and error-prone repair: a model for genomic instability with progression in myeloid leukemia? Cancer Res. 2007;67:8762–8771.
36. Petruccelli LA, Dupéré-Richer D, Pettersson F, Retrouvey H, Skoulikas S, Miller WH Jr. Vorinostat induces reactive oxygen species and DNA damage in acute myeloid leukemia cells. PLoS One. 2011;6:e20987.
37. Li Y, Thrush MA. Diphenyleneiodonium, an NAD(P)H oxidase inhibitor, also potently inhibits mitochondrial reactive oxygen species production. Biochem Biophys Res Commun. 1998;253:295–299.
38. Guaiquil VH, Vera JC, Golde DW. Mechanism of vitamin C inhibition of cell death induced by oxidative stress in glutathione-depleted HL-60 cells. J Biol Chem. 2001;276:40955–40961.
39. Kim JE, Jin DH, Lee SD, et al. Vitamin C inhibits p53-induced replicative senescence through suppression of ROS production and p38 MAPK activity. Int J Mol Med. 2008;22:651–655.
40. de Cássia Yukani Nishimura F, de Almeida AC, Ratti BA, et al. Antioxidant effects of quercetin and naringenin are associated with impaired neutrophil microbicidal activity. Evid Based Complement Alternat Med. 2013;2013:795916.
41. Marks P, Rifkind RA, Richon VM, Breslow R, Miller T, Kelly WK. Histone deacetylases and cancer: causes and therapies. Nat Rev Cancer. 2001;1:194–202.
42. Peart MJ, Smyth GK, van Laar RK, et al. Identification and functional significance of genes regulated by structurally different histone deacetylase inhibitors. Proc Natl Acad Sci USA. 2005;102:3697–3702.
43. Lane AA, Chabner BA. Histone deacetylase inhibitors in cancer therapy. J Clin Oncol. 2009;27:5459–5468.
44. Bots M, Johnstone RW. Rational combinations using HDAC inhibitors. Clin Cancer Res. 2009;15:3970–3977.
45. Garcia-Manero G, Yang H, Bueso-Ramos C, et al. Phase 1 study of the histone deacetylase inhibitor vorinostat (suberoylanilide hydroxamic acid [SAHA]) in patients with advanced leukemias and myelodysplastic syndromes. Blood. 2008;111:1060–1066.
46. Amaru Calzada A, Pedrini O, Finazzi G, et al. Givinostat and hydroxyurea synergize in vitro to induce apoptosis of cells from JAK2(V617F) myeloproliferative neoplasm patients. Exp Hematol. 2013;41:253–260.e2.
47. Carew JS, Gilles FJ, Nawrocki ST. Histone deacetylase inhibitors: mechanisms of cell death and promise in combination cancer therapy. Cancer Lett. 2008;269:7–17.
48. Schieber M, Chandel N. ROS function in redox signaling and oxidative stress. Curr Biol. 2014;24:R453–R462.

49. Walz C, Crowley BJ, Hudon HE, et al. Activated Jak2 with the V617F point mutation promotes G1/S phase transition. J Biol Chem. 2006;281:18177–18183.
50. Wernig G, Gonneville JR, Crowley BJ, et al. The Jak2V617F oncogene associated with myeloproliferative diseases requires a functional FERM domain for transformation and for expression of the Myc and Pim proto-oncogenes. Blood. 2008;111:3751–3759.
51. Marty C, Lacout C, Droin N, et al. A role for reactive oxygen species in JAK2$^{V617F}$ myeloproliferative neoplasm progression. Leukemia. 2013;27:2187–2195.

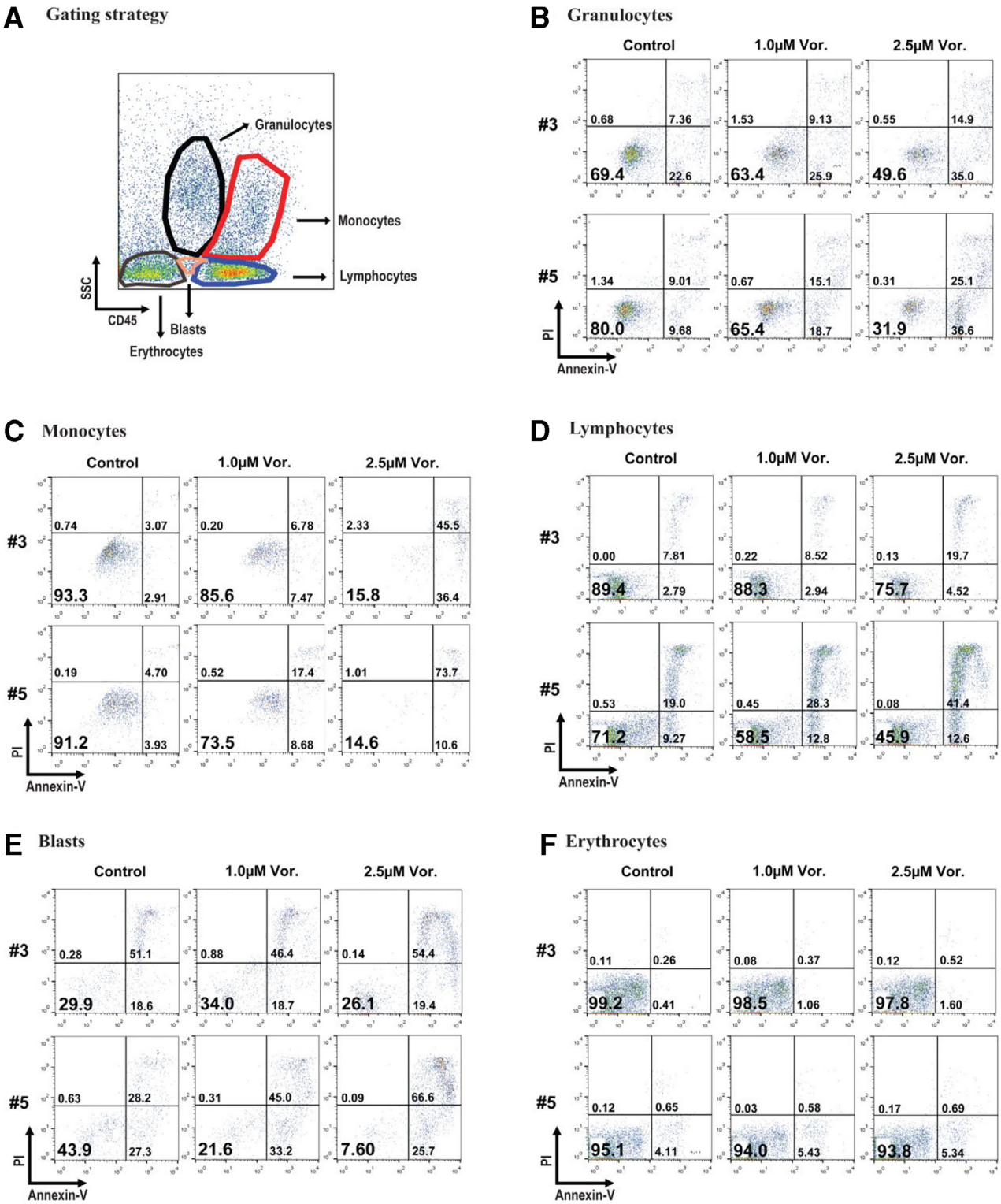


**Supplementary Figure S1. Vorinostat reduces cellular viability in the different lineages of MPN patient samples.** Patient Bone Marrow Mononuclear cells (BMNCs) were isolated by ficoll gradient and cultured with the indicated concentrations of Vor. (Vorinostat). At 72h of culture, the cells were harvested and stained as described in the "Material and Methods" section to determine cellular viability. **A)** Gating strategy [Side Scatter (SSC) vs CD45] to employed to distinguish the different hematopoietic lineages **B)** Granulocytes; **C)** Monocytes; **D)** Lymphocytes; **E)** Blasts and **F)** Erythrocytes. The panels show the Annexin-V/PI dot-plots within the different BMNCs populations of patients #2 and #3.

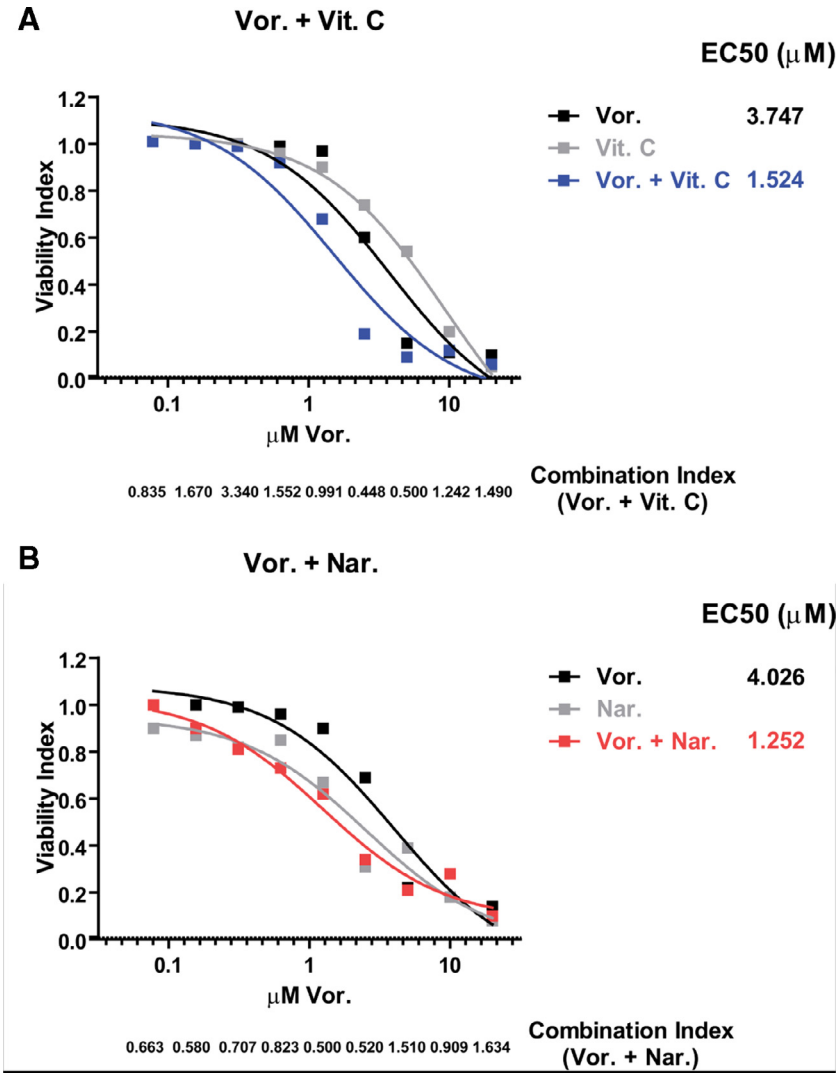


**Supplementary Figure S2. Vorinostat synergizes with Antioxidants to decrease MPN cellular viability.** SET-2 cells were cultured for 72h with increasing concentrations of Vorinostat (Vor.) (10 concentrations ranging from 0.0 to 20.0$\mu$M) that were combined with increasing doses of Vitamin C (Vit. C) (10 concentrations ranging from 0.0 to 10.0mM) **(A)** and Naringenin (Nar.) (10 concentrations ranging from 0.0 to 2000.0$\mu$M) **(B)**. At 72h of co-culture, SET-2 cells were harvested and cellular viability was determined as described in the "Material and Methods" section. The graphics in the panels show the dose response curves of the pharmacological agents in the following conditions: Vor.; Vit. C or Nar. and Vor. + Vit. C or Nar. The EC50 and the Combination Indexes for each drug combinations are show and were calculated as described in "Materials and Methods" section. The data is representative of at least two independent experiments.

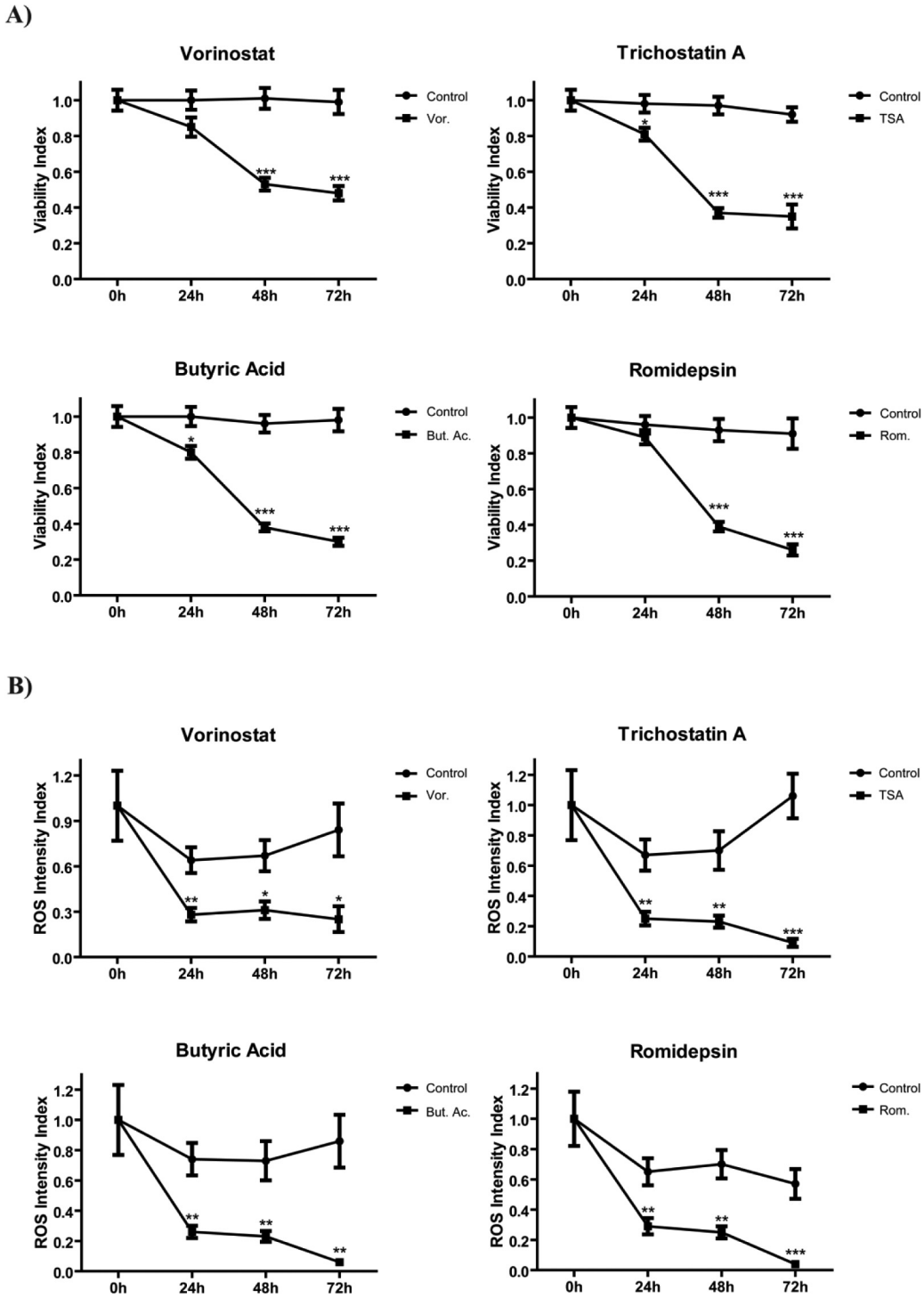


**Supplementary Figure S3. HDAC inhibition reduces MPN cellular viability and intracellular reactive oxygen species (ROS) levels.** SET-2 cells were cultured *in vitro* with several HDAC inhibitors: Vorinostat – 2.5$\mu$M (Vor.); Trichostatin A – 250nM (TSA); Butyric Acid – 1.0mM (But. Ac.) and Romidepsin – 1.0nM (Rom.). At the indicated time points, the cells were harvested and stained as described in the "Material and Methods" section to determine cellular viability **(A)** and intracellular ROS levels **(B)**. The graphics on panels **A** indicate the Viability Index that normalizes the viability values to those of the 0h time point. The graphics on panels **B** indicate ROS Intensity Index that normalizes intracellular ROS levels to those of the 0h time point. Values indicate the mean ± standard deviation of at least three experiments performed (* 0.05>p; ** 0.01>p; *** 0.001>p).

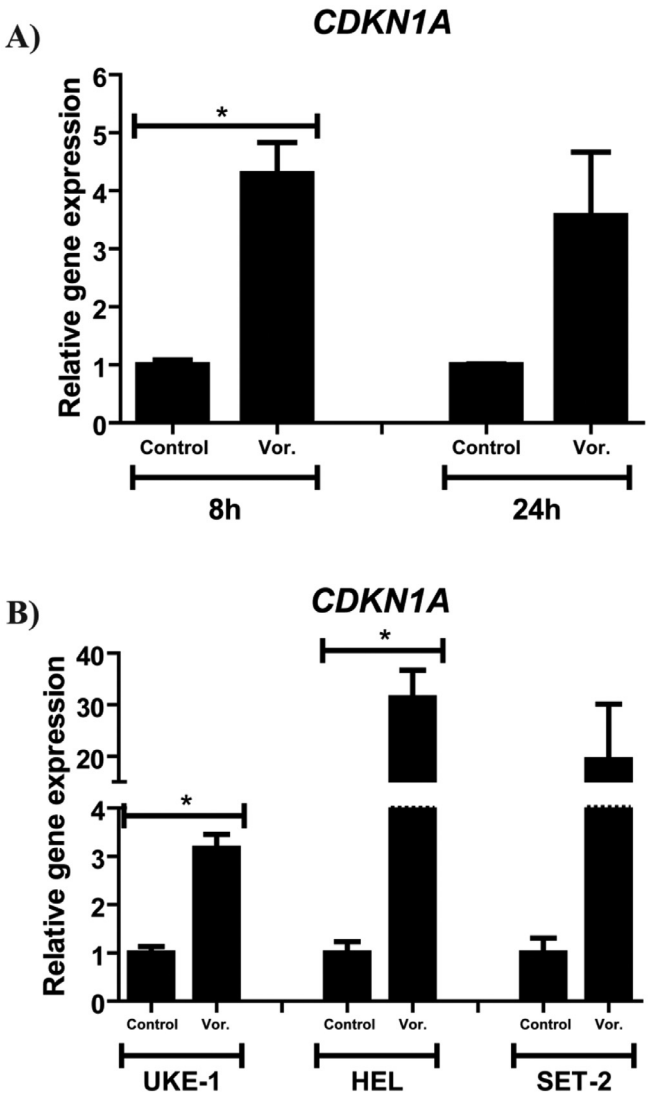


**Supplementary Figure S4. Vorinostat incubation increases *CDKN1A* gene expression. A)** SET-2 cells were cultured in the indicated time points in the presence of Vorinostat (2.5$\mu$M). **B)** The MPN cell lines UKE-1, HEL and SET-2 were culture for 24h in the presence of Vor. (2.0$\mu$M Vorinostat). The transcript levels of *CDK1NA* were evaluated as described in the "Material and Methods" section. The values of each gene were normalized to *HPRT1* and depicted as relative values of the control condition (0.0$\mu$M Vorinostat). The values indicate the mean ± standard deviation of at least three experiments performed (* 0.05>p).

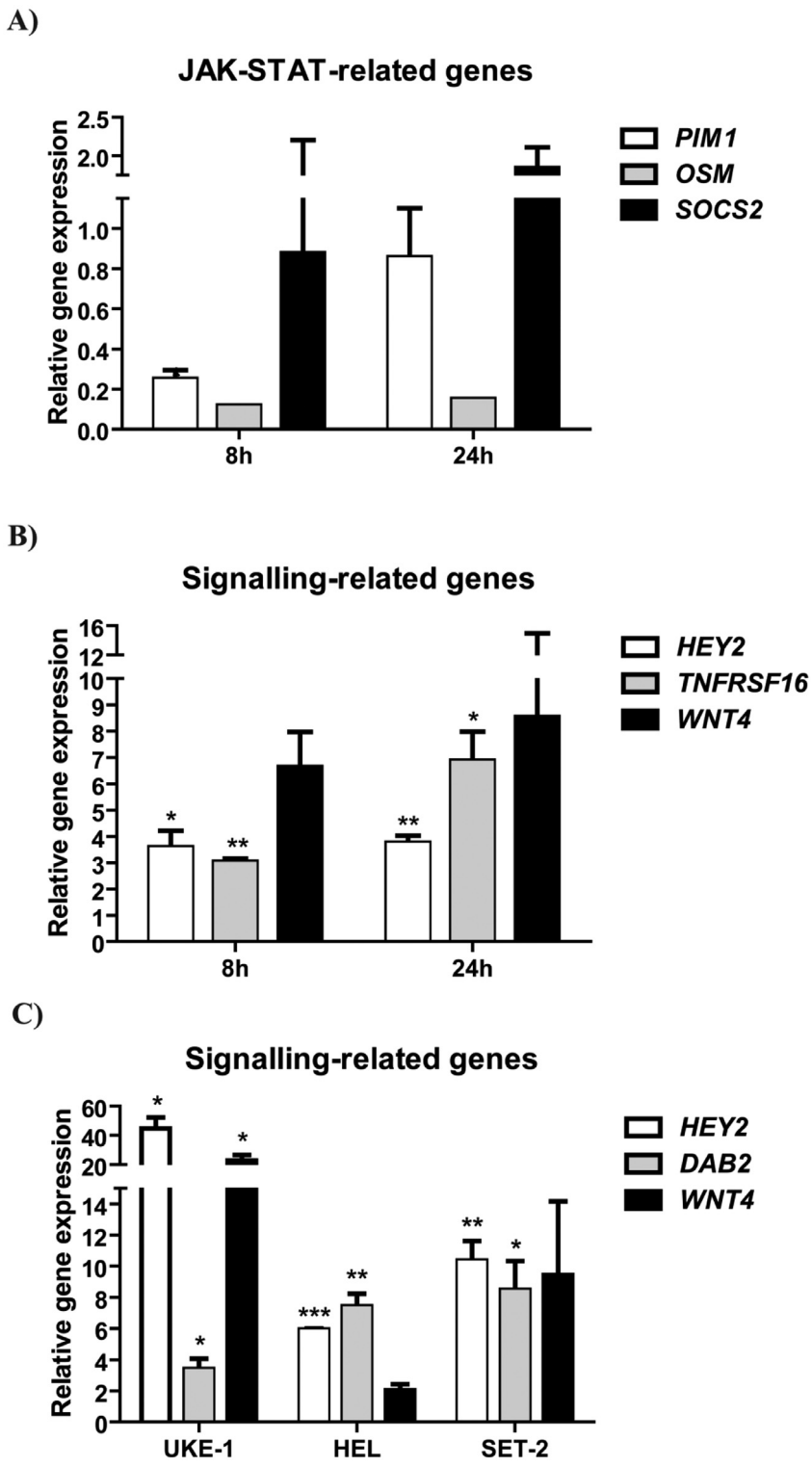


**Supplementary Figure S5. Vorinostat incubation modulates the expression of signalling related genes. A-B)** SET-2 cells were cultured in the indicated time points in the presence of 2.5$\mu$M Vorinostat and the cells were lysed for RNA extraction. **C)** The MPN cell lines UKE-1, HEL and SET-2 were cultured for 24h with 2.0$\mu$M Vorinostat and the cells were lysed for RNA extraction. The transcript levels of the indicated genes were evaluated as described in the "Material and Methods" section. The graphs indicate the values of each gene normalized to *HPRT1* and depicted as relative values of the control condition (0.0$\mu$M Vorinostat). The values indicate the mean ± standard deviation of at least three experiments performed (* 0.05>p; ** 0.01>p; *** 0.001>p).

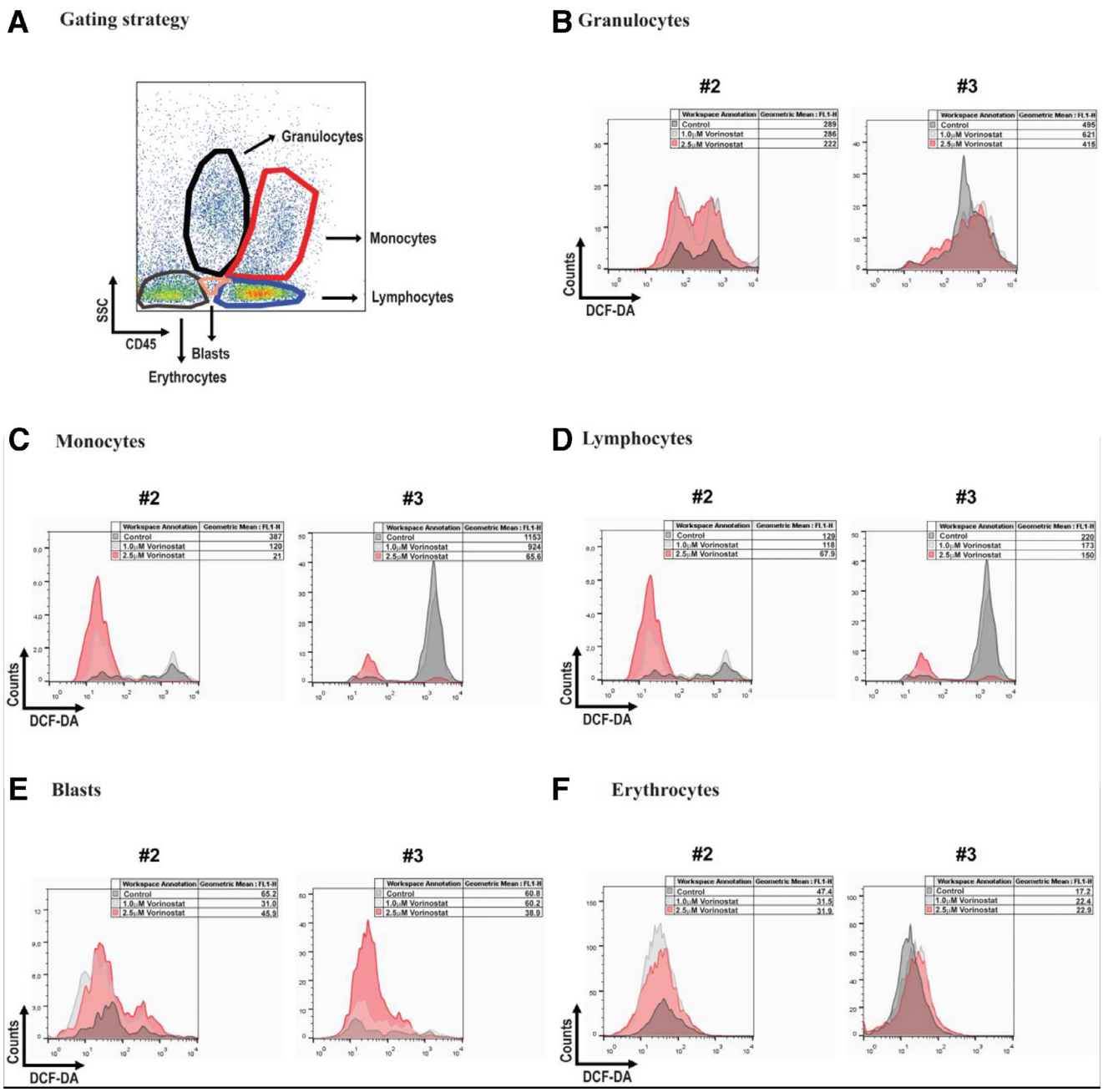


**Supplementary Figure S6. Vorinostat reduces intracellular reactive oxygen species (ROS) levels in the different lineages of MPN patient samples.** Patient Bone Marrow Mononuclear cells (BMNCs) were isolated by ficoll gradient and cultured with the indicated concentrations of Vor. (Vorinostat). At 72h of culture, the cells were harvested and stained as described in the "Material and Methods" section to determine intracellular ROS levels within the different cellular lineages. **A)** Gating strategy [Side Scatter (SSC) vs CD45] to employed to distinguish the different hematopoietic lineages **B)** Granulocytes; **C)** Monocytes; **D)** Lymphocytes; **E)** Blasts and **F)** Erythrocytes. The panels show the histogram-plots of intracellular ROS levels within the different BMNCs populations of patients #2 and #3.

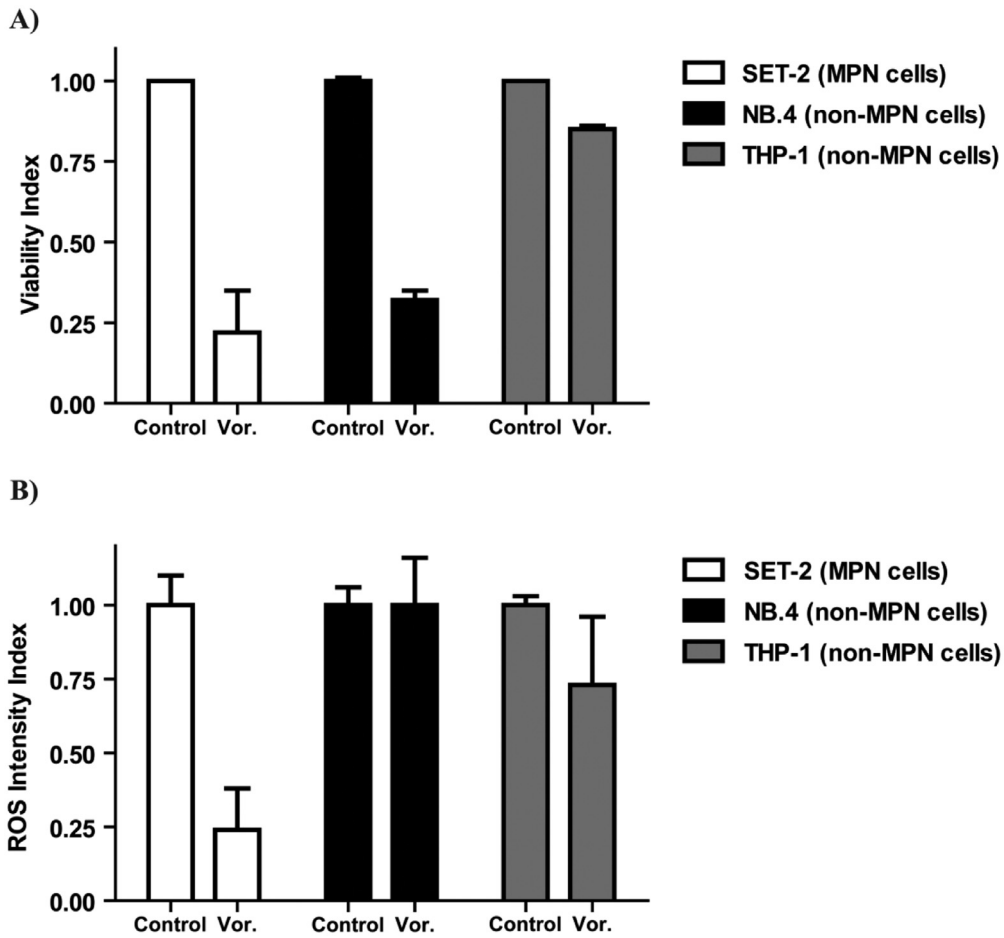


**Supplementary Figure S7. HDAC inhibition reduces cellular viability and intracellular reactive oxygen species (ROS) levels specifically in MPN cells.** SET-2, NB4.1 and THP-1 cells were cultured *in vitro* with Vor. (2.5$\mu$M Vorinostat). At 72h of culture, the cells were harvested and stained as described in the "Material and Methods" section to determine cellular viability **(A)** and intracellular ROS levels **(B)**. The graphics on panels **A** indicate the Viability Index that normalizes the viability values to those of the control conditions (0.0$\mu$M Vorinostat). The graphics on panels **B** indicate ROS Intensity Index that normalizes ROS intracellular levels in the same away as for the Viability Index. Values indicate the mean ± standard deviation of two experiments performed.

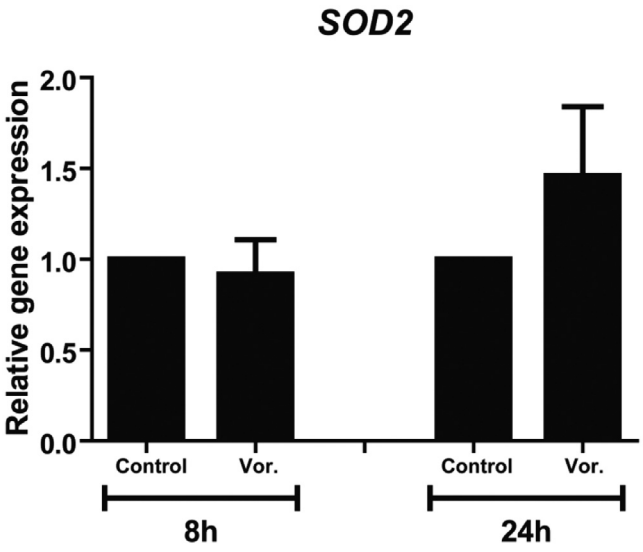


**Supplementary Figure S8. Vorinostat incubation has no effect on *SOD2* gene expression.** SET-2 cells were cultured in the indicated time points in the presence of Vorinostat (2.5$\mu$M). The transcript levels of *SOD2* were evaluated as described in the "Material and Methods" section. The values of each gene were normalized to *HPRT1* and depicted as relative values of the control condition (0.0$\mu$M Vorinostat). The values indicate the mean ± standard deviation of at least three experiments performed.

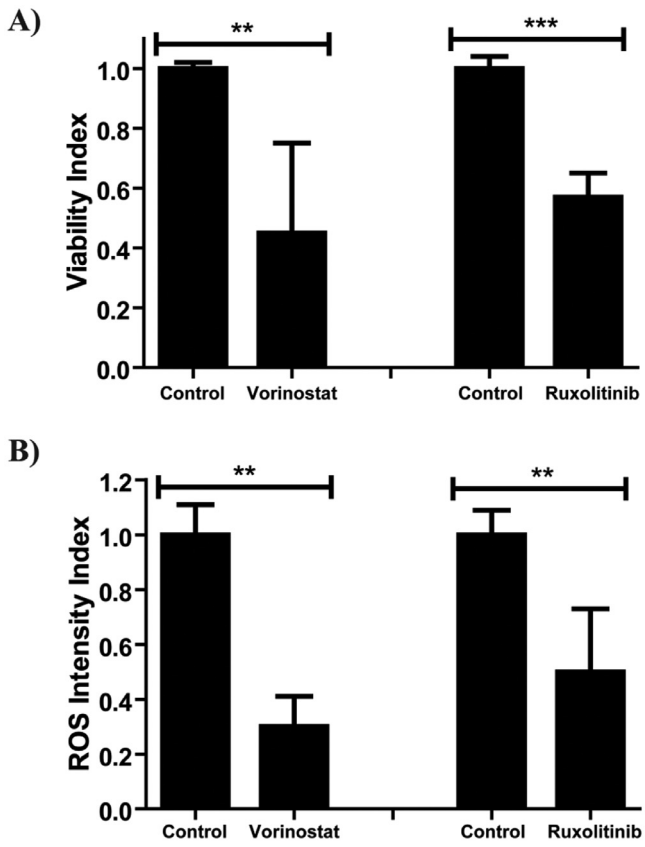


**Supplementary Figure S9. Inhibition of JAK-STAT signalling reduces intracellular reactive oxygen species (ROS) levels in MPN cells.** SET-2 cells were incubated with Vorinostat (2.5$\mu$M) and Ruxolitinib (500nM). At 72h of culture, the cells were harvested and stained as described in the "Material and Methods" section to determine cellular viability **(A)** and intracellular ROS levels **(B)**. The graphics on panels **A** indicate the Viability Index that normalizes the viability values to those of the control conditions (0.0$\mu$M Vor. − left panels; 0nM Rux. − right panels). The graphics on panels **B** indicate ROS Intensity Index that normalizes ROS intracellular levels in the same away as for the Viability Index. Values indicate the mean ± standard deviation of at least three experiments performed (** 0.01>p; *** 0.001>p).

**Supplementary Table S1.** Drug concentrations used to calculated EC50 and drug interaction.

| #1 Vorinostat ($\mu$M) | #2 Ascorbic Acid (mM) | #3 Naringenin ($\mu$M) |
|---|---|---|
| 0.0 | 0.0 | 0.0 |
| 0.078125 | 0.0390625 | 7.8125 |
| 0.15625 | 0.078125 | 15.625 |
| 0.3125 | 0.15625 | 31.25 |
| 0.625 | 0.3125 | 62.5 |
| 1.25 | 0.625 | 125.0 |
| 2.5 | 1.25 | 250.0 |
| 5.0 | 2.5 | 500.0 |
| 10.0 | 5.0 | 1000.0 |
| 20.0 | 10.0 | 2000.0 |

**Supplementary Table S2.** Genes altered by Vorinostat (2.5$\mu$M) upon 8h incubation in SET-2 cells.

| Gene Name | Gene ID (NCBI) | Family/related pathways | Fold induction relative to 0.0$\mu$M Vor. |
|---|---|---|---|
| ***HEY1*** | **23462** | **Kinases, Receptors and Signaling related genes** | **+5.65616** |
| ***TNFRSF16*** | **4804** | **Kinases, Receptors and Signaling related genes** | **+4.73131** |
| ***TNFRSF11A*** | **8792** | **Inflammation** | **+3.58691** |
| ***JAG2*** | **3714** | **Kinases, Receptors and Signaling related genes** | **+3.54881** |
| ***WNT4*** | **54361** | **Kinases, Receptors and Signaling related genes** | **+2.73180** |
| ***CDKN1A*** | **1026** | **Cell Cycle/Proliferation** | **+2.67467** |
| ***HEY2*** | **23493** | **Kinases, Receptors and Signaling related genes** | **+2.44733** |
| ***SERPINB9*** | **5272** | **Apoptosis** | **+2.41231** |
| ***IER3*** | **8870** | **Apoptosis** | **+2.34958** |
| ***SOS1*** | **6654** | **Kinases, Receptors and Signaling related genes** | **+2.07375** |
| ***APAF1*** | **317** | **Apoptosis** | **+1.81061** |
| ***BIM*** | **10018** | **Apoptosis** | **+1.80789** |
| ***TNFRSF21*** | **27242** | **Apoptosis** | **+1.80429** |
| ***FOXO1*** | **2308** | **Transcription factors** | **+1.76356** |
| ***DAB2*** | **1601** | **Kinases, Receptors and Signaling related genes** | **+1.60421** |
| ***CIITA*** | **4261** | **Transcription factors** | **-1.26277** |
| ***NBN*** | **4683** | **Cell Cycle/Proliferation** | **-1.37397** |
| ***TAL1*** | **6886** | **Transcription factors** | **-1.80742** |
| ***LMO2*** | **4005** | **Transcription factors** | **-1.97150** |
| ***PIM1*** | **5292** | **Kinases, Receptors and Signaling related genes** | **-1.99948** |
| ***MZF1*** | **7593** | **Transcription factors** | **-2.48379** |
| ***OSM*** | **5008** | **Kinases, Receptors and Signaling related genes** | **-3.08000** |

**Supplementary Table S3.** A Genes altered by Vorinostat (2.5$\mu$M) upon 24h incubation in SET-2 cells.

| Gene Name | Gene ID | Family/related pathways | Fold Induction relative to 0.0$\mu$M Vor. |
|---|---|---|---|
| ***IER3*** | **8870** | **Apoptosis** | **+6.83463** |
| ***JAG2*** | **3714** | **Kinases, Receptors and Signaling related genes** | **+6.64386** |
| ***TNFRSF16*** | **4804** | **Kinases, Receptors and Signaling related genes** | **+6.06655** |
| ***HEY1*** | **23462** | **Kinases, Receptors and Signaling related genes** | **+5.30844** |
| ***BIRC3*** | **330** | **Apoptosis** | **+5.24307** |
| ***TNFRSF11A*** | **8792** | **Inflammation** | **+4.49466** |
| ***BCL6*** | **604** | **Apoptosis** | **+4.45533** |
| ***GRAVIN*** | **5590** | **Kinases, Receptors and Signaling related genes** | **+3.93238** |
| ***MAPK8IP2*** | **23542** | **Kinases, Receptors and Signaling related genes** | **+3.75298** |
| ***BIRC2*** | **329** | **Apoptosis** | **+3.29132** |
| ***GADD45B*** | **4616** | **Cell Cycle/Proliferation** | **+3.28530** |
| ***WNT4*** | **54361** | **Kinases, Receptors and Signaling related genes** | **+3.28048** |
| ***HDAC11*** | **79885** | **Chromatin remodeling and DNA repair** | **+3.27272** |
| ***FOXO1*** | **2308** | **Transcription factors** | **+3.25084** |
| ***TNFRSF9*** | **3604** | **Apoptosis** | **+3.19171** |
| ***CJUN*** | **3725** | **Cell Cycle/Proliferation** | **+3.14881** |
| ***CFOS*** | **2353** | **Cell Cycle/Proliferation** | **+2.97234** |
| ***IL8*** | **3576** | **Inflammation** | **+2.89394** |
| ***CD40*** | **958** | **Inflammation** | **+2.86810** |
| ***AXL*** | **558** | **Kinases, Receptors and Signaling related genes** | **+2.83662** |
| ***DAB2*** | **1601** | **Kinases, Receptors and Signaling related genes** | **+2.78262** |
| ***JUNB*** | **3726** | **Cell Cycle/Proliferation** | **+2.74087** |
| ***JAG1*** | **182** | **Kinases, Receptors and Signaling related genes** | **+2.67773** |
| ***TNFRSF10C*** | **8794** | **Apoptosis** | **+2.59039** |
| ***COX2*** | **5743** | **Inflammation** | **+2.49033** |
| ***BIM*** | **10018** | **Apoptosis** | **+2.42444** |
| ***HIP1*** | **3092** | **Kinases, Receptors and Signaling related genes** | **+2.41227** |
| ***CDKN1A*** | **1026** | **Cell Cycle/Proliferation** | **+2.40042** |
| ***TNFRSF21*** | **27242** | **Apoptosis** | **+2.26920** |
| ***CCNG2*** | **901** | **Cell Cycle/Proliferation** | **+2.22415** |
| ***IFT57*** | **55081** | **Apoptosis** | **+2.10350** |
| ***PAK1*** | **5058** | **Kinases, Receptors and Signaling related genes** | **+2.07077** |
| ***HEY2*** | **23493** | **Kinases, Receptors and Signaling related genes** | **+1.91015** |
| ***HES1*** | **3280** | **Kinases, Receptors and Signaling related genes** | **+1.90904** |
| ***FOXL2*** | **668** | **Transcription factors** | **+1.87069** |
| ***APAF1*** | **317** | **Apoptosis** | **+1.80919** |
| ***IFI6*** | **2537** | **Apoptosis** | **+1.70308** |
| ***NOTCH2*** | **4853** | **Kinases, Receptors and Signaling related genes** | **+1.64949** |
| ***SOS1*** | **6654** | **Kinases, Receptors and Signaling related genes** | **+1.63180** |
| ***RNF20*** | **56254** | **Kinases, Receptors and Signaling related genes** | **+1.53999** |
| ***ERG*** | **2078** | **Transcription factors** | **+1.51036** |
| ***PRKCA*** | **5578** | **Kinases, Receptors and Signaling related genes** | **+1.44157** |
| ***ETS2*** | **2114** | **Transcription factors** | **+1.36533** |
| ***ETS1*** | **2113** | **Transcription factors** | **+1.24589** |
| ***DDAH2*** | **23564** | **Metabolism** | **+1.15429** |
| ***GFI1B*** | **8328** | **Transcription factors** | **+1.41795** |
| ***STAT2*** | **6773** | **Kinases, Receptors and Signaling related genes** | **+1.21120** |
| ***HDAC10*** | **83933** | **Chromatin remodeling and DNA repair** | **+1.18280** |
| ***TAL1*** | **6886** | **Transcription factors** | **+1.13675** |
| ***OSM*** | **5008** | **Kinases, Receptors and Signaling related genes** | **-1.40382** |

**Supplementary Table S4.** List of genes analyzed in the screen.

| Family /related pathways | Genes |
|---|---|
| **Apoptosis** | ***APAF1, BAD, BAX, BCLXL, BCL2, BCL6, BIM, BIRC2, BIRC3, CARD9, CASP9, FASLG, IER3, IFI6, IFT57, PPP1R13B, SERPINB9, TNFRSF1A, TNFRSF6, TNFRSF6B, TNFRSF8, TNFRSF9, TNFRSF10A, TNFRSF10B, TNFRSF10C, TNFRSF10D, TNFRSF12A, TNFRSF16, TNFRSF21, TNFRSF25, TP53, XIAP*** |
| **Cell Cycle/Proliferation** | ***ANAPC2, CCND1, CCND2,CCNDG2, CDKN1A, CDK4, CDK6, CFOS, CJUN, CMYC, FOSL2, GADD45B, JUNB, NBN,NRAS, PCNA, RAD9A,*** |
| **Kinases, Receptors and Signaling related genes** | ***AURKC, AXIN1, AXL, BTRC, CTNNB1, CUL1, DAB2, EGR1, ERS1, GRAVIN, GSK3B, HES1, HES5, HEY1, HEY2, HIP1, HSPA5 IL7RA, JAG1, JAG2,JAK2, LEF1, MAPK8IP2, MTSS1, NOTCH2, OSM, PAK1, PIASY, PIM1,PI3KCA, PKB, PRKCA, PTEN, RASA1, RFN20, SEMA4D, SHIP1, SMAD1, SMAD2, SMAD3, SMAD4, SOCS2, SOS1, STAT2, STAT5A, STIP1, TNFRSF16, WNT3, WNT4*** |
| **Inflammation** | ***CD40, COX2, CREL, CSF1, ID1, IFI6, ILF3, IL1β, IL8, LTBR, MYD88, NFKB1, RELA, TNFRSF11A, TNFRSF14, TNFRSF25*** |
| **Metabolism** | ***DDAH2,MNSOD, NOS2*** |
| **Chromatin remodeling and DNA repair** | ***DNMT1, DNMT3B, EP300, EZH2, FANCA, FANCB, FANCC, FANCD1, FANCD2, FANCE, FANCF, FANCG, FANCJ, FANCL, FANCM, FANCN, FANCO, FANCP, HDAC8, HDAC10, HDAC11, SETD6, USP16,*** |
| **Transcription factors** | ***ATF2, CIITA, ERG, ERS1, ETS1,ETS2, FOXL2, FOXO1, FOXO3A, GATA1, GATA2, GFI1B, ID1, LMO2, MCL1, MEF2C, MZF1, RUNX1, RUNX3, SP1, TAL1*** |